EAST EUROPEAN JOURNAL OF PHYSICS. 4. 43-48 (2021)
DOI: 10.26565/2312-4334-2021-4-04 ISSN 2312-4334

ELECTRICAL AND PHOTOELECTRIC PROPERTIES OF ORGANIC-INORGANIC HETEROJUNCTIONS PEDOT:PSS/*n*-CdTe[†]

Hryhorii P. Parkhomenko[a], Mykhailo M. Solovan[a], Andrii I. Mostovyi[a], Ivan G. Orletskyi[a], Viktor V. Brus[b,*]

[a]*Department of Electronics and Energy Engineering, Chernivtsi National University, 58012, Chernivtsi, Ukraine*
[b]*Department of Physics, Nazarbayev University, 010000, Nur-Sultan, Kazakhstan*
**Corresponding Author: viktor.brus@nu.edu.kz*
Received September 28, 2021; accepted November 14, 2021

PEDOT: PSS thin films are widely used as transparent coatings in flexible semiconductor devices including solar cells. However, they are not widely used as transparent coatings in combination with crystal substrates. This work shows the possibility of using PEDOT:PSS thin films as a frontal transparent conducting layer in hybrid organic-inorganic Schottky type heterojunctions of the PEDOT:PSS/*n*-CdTe, which were prepared by deposition of PEDOT:PSS thin films (using the spin-coating method) on crystalline cadmium telluride substrates. The current-voltage (in a wide temperature range) and capacitance-voltage (at room temperature) characteristics of heterojunctions were measurement and analyzed. It has been established that PEDOT:PSS/*n*-CdTe heterojunctions have good diode properties with a high rectification ratio RR≈10^5, a potential barrier height φ_0 = 0.95 eV, and series R_s = 91 Ohm and shunt R_{sh} = 5.7 × 10^7 Ohm resistances. Analysis of the forward branches of the *I–V* characteristics of heterojunctions showed that the dominant charge transfer mechanisms are determined by the processes of radiative recombination at low biases (3kT/e <*V* <0.3 V) and tunneling through a thin depleted layer at high biases (0.3 V <*V* <0.6 V). Capacity-voltage characteristics are plotted in the Mott-Schottky coordinate, taking into account the influence of series resistance, measured at a frequency of 1 MHz. Used the C-V characteristic was determined the value of the built-in potential V_c = 1.32 V (it correlates well with the cutoff voltage determined from the current-voltage characteristics) and the concentration of uncompensated donors in the *n*-CdTe substrate N_D-N_A = 8.79 × 10^{14} cm^{-3}. Although the photoelectric parameters of unoptimized PEDOT:PSS/*n*-CdTe heterojunctions are low, their photodiode characteristics (Detectivity D^*> 10^{13} Jones) are very promising for further detailed analysis and improvement. The proposed concept of a hybrid organic-inorganic heterojunction also has potential for use in inexpensive γ- and X-ray detectors.
Keywords: PEDOT:PSS, CdTe, heterojunction, photodetector, current transport.
PACS: 68.65.Pq, 68.55.Jk, 68.37.Hk, 68.37.−d, 71.20.−b, 71.20.Nr

For a long time, many scientific laboratories have been developing the technology to obtain high-quality crystals of cadmium telluride CdTe and study their physical properties. This material attracts materials scientists and device engineers involved in the development of new types of semiconductor devices for various applications.

Cadmium telluride (CdTe) is a direct-gap semiconductor of the $A^{II}B^{VI}$ group with a wide bandgap of 1.49 eV at 300 K [1,2]. Currently, CdTe semiconductor crystals find their application in different optoelectronic devices: solar cells, lasers, photoresistors, and ionizing radiation detectors [3-5].

Among the conductive polymers, PEDOT:PSS (polyenidoxythiophene) is widely used in organic and hybrid perovskite optoelectronics [6,7]. It can also replace transparent conductors such as ITO or FTO and is widely used on flexible substrates [8-10]. This degenerated p-type organic semiconductor is particularly interesting due to the synergy of its optical and electrical properties with the advantages of simple, low-cost solution processing.

So far, PEDOT:PSS films were used to fabricate ohmic back contacts to CdTe thin-film solar cells [11]. This is possible because of the large work function of PEDOT:PSS films close to that of p-type CdTe.

This contribution is the first to report on employing PEDOT:PSS thin films as the front transparent functional layer in a Schottky-type hybrid organic-inorganic heterojunction PEDOT:PSS/n-CdTe.

EXPERIMENTAL DETAILS

The heterojunctions were fabricated by spin-coating PEDOT:PSS water suspension at room temperature on freshly cleaved *n*-CdTe substrates (3.5×3.5×0.7 mm^3) at 2000 rpm. Afterward, the samples were annealed in air at the temperature of 370 K.Properties of the CdTe crystals are described in our previous paper [12].

The front electric contact to the PEDOT:PSS thin films was formed by using a graphite conductive paste. During the formation of the back electrical contact to the single-crystal n-CdTe substrate, a copper layer was deposited via the reduction from an aqueous solution of copper sulfate, followed by the thermal evaporation of indium [13].

A schematic representation of the fabricated photosensitive hybrid organic-inorganic heterostructures PEDOT:PSS/*n*-CdTe is shown in Figure 1a. The energy diagram of the PEDOT:PSS/n-CdTe heterojunction, built according to the Anderson model [14] is shown in Figure 1b. The energy parameters of the semiconductor components of the heterojunction were taken from the literature [5,14-17].

[†] ***Cite as:*** H.P. Parkhomenko, M.M. Solovan, A.I. Mostovyi, I.G. Orletskyi, and V.V. Brus, East. Eur. J. Phys. **4**, 43 (2021), https://doi.org/10.26565/2312-4334-2021-4-04

The current-voltage characteristics of the heterojunctions were measured according to the standard method using a Keysight B2985A precision Femto/pico-amperemeter in combination with a voltmeter Agilent 34410A. The measurements of the capacitance-voltage (*C–V*) characteristics of the heterojunctions were completed by an LCR Meter BR2876.

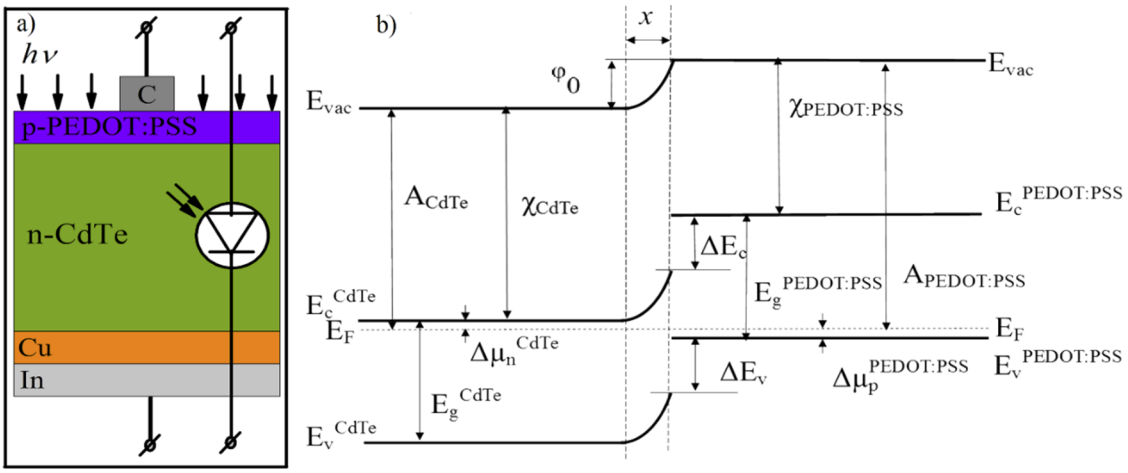

Figure 1. a) a schematic representation of the PEDOT:PSS/n-CdTe heterojunction photodiode; b) energy diagram of the PEDOT:PSS/n-CdTe heterojunction at zero bias: $E_g^{PEDOT:PSS} = 1.6$ eV, $\chi_{PEDOT:PSS} = 3.6$ eV, $A_{PEDOT:PSS} = 5.1$ eV, $E_g^{CdTe} = 1.5$ eV, $\chi_{CdTe} = 4.28$ eV, $A_{CdTe} = 4.38$ eV $\Delta\mu_p^{PEDOT:PSS} \approx 0.1$ eV, $\Delta\mu_n^{CdTe} = 0.1$ eV, $\Delta E_c = 0.68$ eV, $\Delta E_v = 0.58$ eV, $\varphi_0 = 0.72$ eV.

RESULTS AND DISCUSSIONS

Electrical properties of the PEDOT:PSS/n-CdTe heterostructures

Figure 2a reveals dark current-voltage characteristics of the hybrid heterojunctions PEDOT:PSS/n-CdTe. The work function difference between the PEDOT:PSS (5.1 eV) [17] and n-CdTe (4.38 eV) [5] resulted in a potential barrier for charge transport at the heterojunction interface with a high rectification ratio $RR_{2V} = 10^5$.

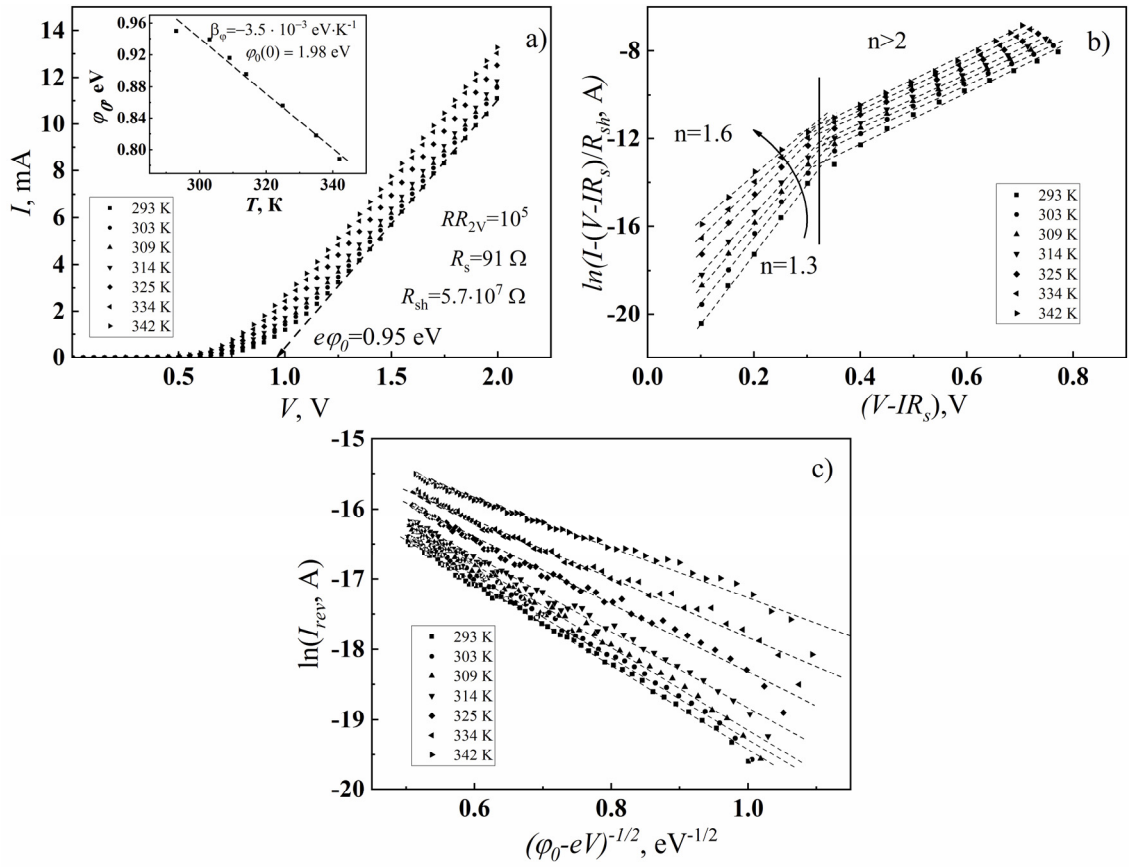

Figure 2. a) *I-V* characteristics of the PEDOT:PSS/*n*-CdTe heterojunctions (the inset: temperature dependence of the potential-barrier height); b) Forward branch of the *I–V* characteristics in a semi-logarithmic scale, taking into account the effect of series and shunt resistance; c) The tunneling current transport through the heterojunction under investigation at reverse bias.

Extrapolating the linear parts of the *I–V* characteristics towards their interception with the voltage axis allows to determine the height of the potential barrier at the PEDTO:PSS/n-CdTe heterojunction interface at different temperatures $\varphi_0 = eV_{bi}$, where V_{bi} is the built-in voltage, (see the inset in Fig. 2a). We have found that the temperature dependence of the potential-barrier height at the PEDOT:PSS/n-CdTe heterojunction is well described by the linear equation [12]:

$$\phi_0(T) = \phi_0(0) - \beta_\phi \cdot T \,, \tag{1}$$

where β_φ = -3.5 · 10^{-3} eV/K is the temperature coefficient of the potential-barrier height and $\varphi_0(0)$ = 1.98 eV is the potential-barrier height of the investigated heterojunction at the absolute zero temperature.

The series resistance R_s = 91 Ohm and shunt resistance R_{sh}=5.7·10^7 Ohm of the organic-inorganic heterojunction photodiode PEDOT:PSS/*n*-CdTe were established from the voltage dependence of its differential resistance R_{dif} at room temperature [18,19].

Charge transport mechanisms

Figure 2b shows the forward branches of the *I–V* characteristics of the hybrid PEDOT:PSS/*n*-CdTe heterojunction in the semi-logarithmic scale $\ln[I-(V-IR_s)/R_{sh}] = f(V-IR_s)$. The plot consists of two linear sections, that indicates an exponential dependence of current on voltage and the presence of two dominant charge transport mechanisms within the considered voltage range. The values of the ideality factor *n* ($\Delta\ln[I-(V-IR_s)/R_{sh}]/\Delta(V-IR_s) = e/nkT$) [20,21] for two voltage regions are shown in Figure 2b.

First, consider the voltage range ($3kT/e<V<0.3$ V). In this range, the measured *I–V* characteristics can be governed by the standard equation, which takes into account the effect of the series R_s and shunt R_{sh} resistance [22]:

$$I = I_0\left[\exp\left(\frac{e(V - IR_s(T))}{nkT}\right) - 1\right] + \frac{V - IR_s(T)}{R_{sh}(T)}\,, \tag{2}$$

where I_0 is the saturation current, *n* is the ideality factor, *k* is the Boltzmann constant and *T* is the absolute temperature.

The value of the nonideality factor changes from 1 to 2 with increasing temperature, which suggests that the current in this voltage range is well described by the emission-recombination model of current transport [15,20].

Now let us consider linear sections in the voltage range $V > 0.3$ V. The large nonideality factor $n > 2$ provides evidence on the tunneling model of charge transport. At large forward bais the space charge region becomes thin enough for direct tunneling and the *I–V* characteristics are well described by the Newman formula [12,14]:

$$I = I_t^0 \exp(\gamma T)\exp\left[\alpha(V - IR_s)\right] = I_t \exp\left[\alpha(V - IR_s)\right], \tag{3}$$

where I_t^0=2.3 · 10^{-12} A, α=11.8 eV, γ = 3.7 ·10^{-2} $K^{-1}$are constants.

In the case of an abrupt junction, the expression for the tunneling current at reverse bias has the form (4). Therefore, according to equation (4), the appearance of the reverse branches of the *I-V* characteristics as straight lines in the coordinates $\ln I_{rev} = f((\varphi_0 - qV)^{-1/2}$ (Figure 2c) confirms the dominance of the tunneling mechanism of current transport at reverse bias [23].

$$I_{rev} \approx a_0 \exp\left(\frac{b_0}{\sqrt{\phi_0(T) - eV}}\right) \tag{4}$$

where a_0 and b_0 are the voltage-independent parameters.

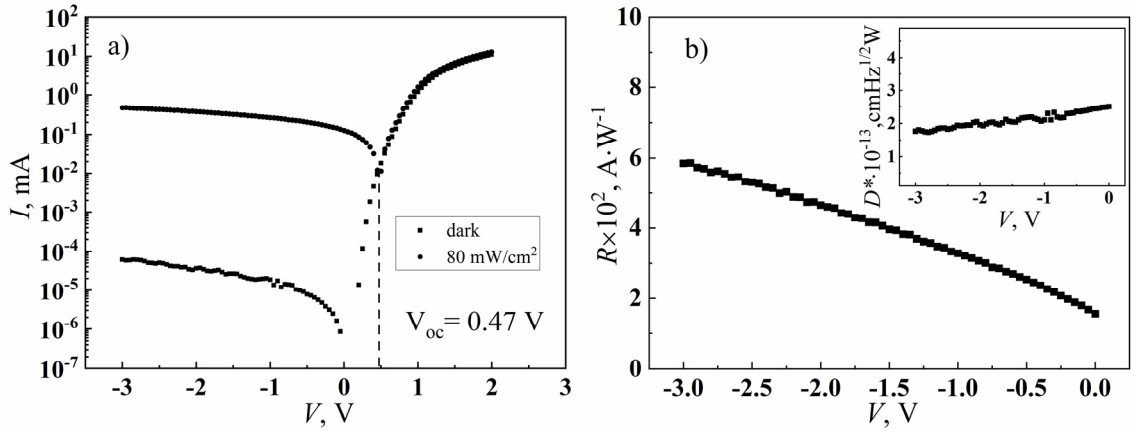

Figure 3. a) *I-V* characteristic of the PEDOT:PSS/*n*-CdTe heterojunction in the dark and under the white light illumination with the intensity of 80 mW/cm^2; b) voltage dependence of responsivity (*R*). The inset reveals the voltage dependence of detectivity (*D**).

Photoelectric properties

Figure 3a reveals the dark and light *I-V* characteristics of the hybrid heterojunction PEDOT:PSS/*n*-CdTe. The photovoltaic parameters of the heterojunction are the following: open-circuit voltage V_{oc} = 0.47 V, short-circuit current I_{sc} = 1.3 mA/cm^2, and fill factor FF = 0.31 under white light illumination with the intensity of 80 mW/cm^2.

The photodiode characteristics of the heterojunction can be quantified via its responsivity (R) and detectivity (D^*) in the shot noise-limited case [24,25]:

$$R=(I_{light}-I_{dark})/P_{opt}, \quad (5)$$

$$D^*=(RS/2qI_{dark})^{1/2}, \quad (6)$$

Where S is the photodetector area.

The responsivity R increases at larger reverse bias due to the widening of the depletion region, thus, improving the efficiency of separating photoinduced charge carriers (see Fig. 3b). The specific detectivity D^* describes the normalized radiation power required to obtain a signal from the photodetector at the noise level, remains relatively constant within the all tested range of reverse bias due to the counter compensating between the increasing I_{dark} and increasing R.

C-V characteristics

Figure 4a shows the capacitance-voltage characteristics of the hybrid heterojunction PEDOT:PSS/*n*-CdTe, the measurements were carried out at room temperature, in the frequency range 20 kHz - 1 MHz in the parallel RC circuit mode, the alternating current amplitude was 20 mV. Since part of the applied DC bias is dropped across the series resistance, so its effect was accounted for as follows: $V_{cor}=V-IR$.

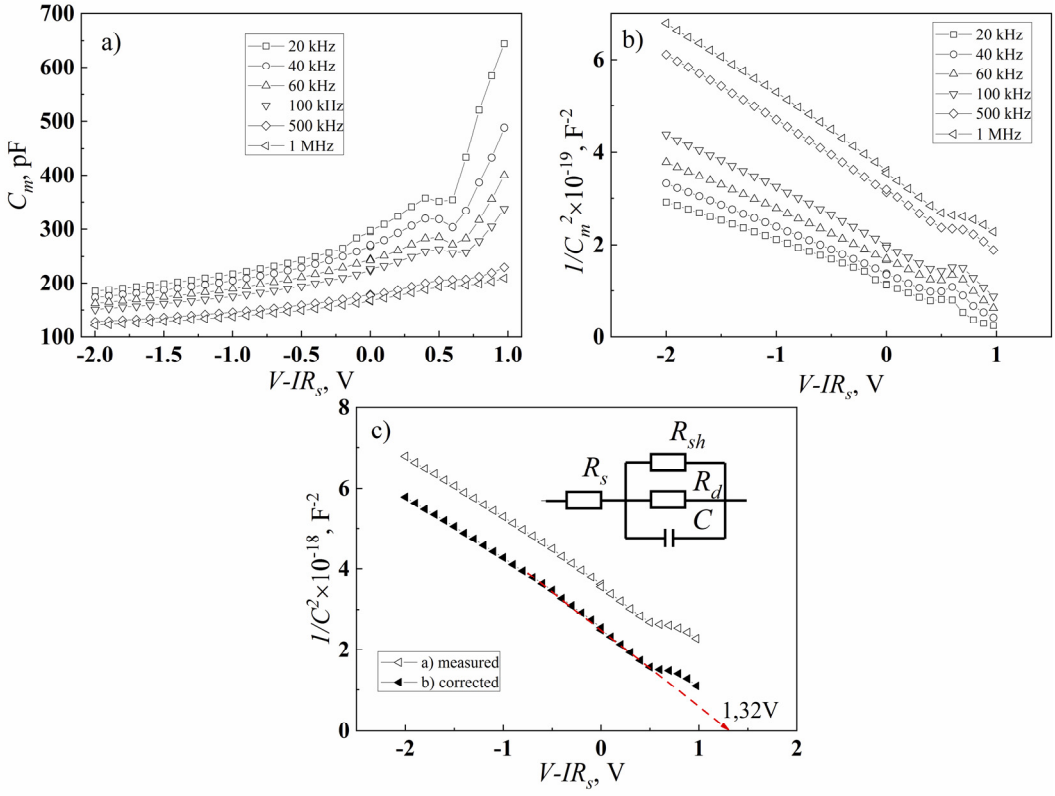

Figure 4. a) *C-V* characteristics of PEDOT:PSS/*n*-CdTe heterojunction at room temperature b) *C-V* characteristics in Mott-Schottky coordinates; c) Mott-Schottky dependence, measured at the frequency of 1 MHz: measured capacitance C_m, corrected capacitance by the effect of the series resistance C.

Let us consider the frequency dependence of the measured capacitance-voltage characteristics. It was shown in [26,27] that surface and bulk traps affect the measured capacitance C_m only at low frequencies while they can still follow the AC test signal. Thus, measuring C-V characteristics at high frequencies can mitigate the excessive capacitance originated from charging and discharging traps. At the same time, the series resistance parasitic contribution to the measured capacitance becomes more apparent with the increase of frequency (Fig. 4a). Therefore, the increase of the slope of the Mott-Schottky dependence in the frequency range 20 – 500 kHz dominantly results from the reduced capacitance originated from the charging-discharging surface and bulk traps. However, in the high-frequency range 500 kHz – 1 MHz, the parallel shift of the Mott-Schottky dependence is caused almost purely by the parasitic effect of the series resistance (Fig. 4b).

Since the effect of traps is negligible at the high frequency of 1 MHz, it is possible to analyze the *C-V* characteristics in this frequency range using a simplified equivalent circuit (the inset in Fig. 4c). The barrier capacitance of the heterojunction is calculated using the following formula, which accounts for the parasitic effect of the series resistance on measured high-frequency capacitance[27]:

$$C = \left[\frac{C_m^{-2} - 2R_s^2\omega^2 - \sqrt{\left(C_m^{-2} - 2R_s^2\omega^2\right)^2 - 4R_s^4\omega^4}}{2R_s^4\omega^4} \right]^{1/2}. \quad (7)$$

Plotting the high-frequency Mott-Schottky dependence, corrected by the effect of the series resistance (Fig. 4c), allows proper analysis of the height of the potential barrier and the concentration of uncompensated donor centers in the CdTe substrate. By extrapolating the linear part of the corrected Mott-Schottky dependence toward the intersection with the voltage axis, we determine the value of the built-in potential $V_c = 1.32$ V that is in good agreement with the value of the built-in potential determined from the *I–V* characteristic of the heterojunctions $V_{bi} = 1.32$ V.

According to the Donelly-Milns model [28], this is clear evidence of a high-quality heterojunction interface between the PEDOT:PSS layer and the n-CdTe substrate without charged interface defect states.

Having taken into account that the space charge region is almost entirely located in the CdTe substrate, the voltage dependence of the barrier capacitance can be expressed by the following equation [13]:

$$C = S\sqrt{\frac{e^2\varepsilon_n\varepsilon_0 N_D - N_A}{2\left(\phi_0 - e(V - IR_s)\right)}}, \quad (8)$$

Where S is the area of the heterojunction.

The density of uncompensated donors can be determined from the slope of the Mott-Schottky dependence [13]:

$$N_D - N_A = -\frac{2}{S^2 e\varepsilon_n\varepsilon_0 \dfrac{\Delta C^{-2}}{\Delta(V - IR_s)}}. \quad (9)$$

The determined densities of uncompensated donors in the base material for linear regions at a reverse bias (Figure 4c) are 8.79×10^{14} cm^{-3}.

CONCLUSION

The possibilities of using solution-processed PEDOT:PSS thin films for the fabrication of photosensitive hybrid organic-inorganic heterojunctions PEDOT:PSS/n-CdTe were experimentally revealed in this study.

It was established that PEDOT:PSS/*n*-CdTe heterojunctions possess quite decent diode properties with a high rectification ratio $RR \approx 10^5$, the height of the potential barrier $\varphi_0 = eV_{bi} = 0.95$ eV and the values of the series $R_s = 91$ Ω and shunt resistance $R_{sh} = 5.7 \cdot 10^7$ Ω.

The analysis of the forward branches of the *I–V* characteristics of the heterojunctions has shown that the dominant mechanisms of charge transport are defined by emission-recombination processes at a low bias ($3kT$ / e < V < 0.3 V) and tunneling through the thin depletion layer at large bias (0.3 V < V < 0.6 V).

Mott-Schottky dependence, measured at the frequency of 1 MHz and corrected by the effect of the series resistance, was used to determine the built-in potential $V_c = 1.32$ V (in good correlation with the cut-off voltage of the measured *I-V* characteristics) and the concentration of uncompensated donors in the n-CdTe substrate N_D-$N_A = 8.79\times10^{14}$ cm^{-3}.

Although the photovoltaic parameters of the unoptimized PEDOT:PSS/*n*-CdTe heterojunctions are low, their photodiode performance is quite promising for further detail analysis and improvement. The proposed concept of a hybrid wide-bandgap organic-inorganic solution-processed Schottky-type heterojunction also has potential for applications in low-cost γ- and *x*-ray detectors [29].

ORCID IDs

Hryhorii P. Parkhomenko, https://orcid.org/0000-0001-5358-1505; **Mykhailo M. Solovan,** https://orcid.org/0000-0002-1077-5702
Andrii I. Mostovyi, https://orcid.org/0000-0001-9634-0058; **Ivan G. Orletskyi,** https://orcid.org/0000-0001-5202-8353
Viktor V. Brus, https://orcid.org/0000-0002-8839-124X

REFERENCES

[1] P. Handler, Science **159**, 185 (1968). https://doi.org/10.1126/science.159.3811.185
[2] H. Lin, Irfan, W. Xia, H.N. Wu, Y. Gao, and C.W. Tang, Solar Energy Materials and Solar Cells, **99**, 349 (2012). https://doi.org/10.1016/j.solmat.2012.01.001
[3] Y. Eisen, and A. Shor, Journal of Crystal Growth, **184–185**, 1302 (1998), https://doi.org/10.1016/S0022-0248(98)80270-4
[4] V.V. Brus, and P.D. Maryanchuk, Carbon **78**, 613 (2014), https://doi.org/10.1016/j.carbon.2014.07.021
[5] H. Parkhomenko, M. Solovan, V.V. Brus, E. Maystruk, and P.D. Maryanchuk, OE, **57**, 017116 (2018), https://doi.org/10.1117/1.OE.57.1.017116

[6] I.B. Olenych, O.I. Aksimentyeva, L.S. Monastyrskii, Y.Y. Horbenko, and L.I. Yarytska, Nanoscale Res Lett, **10**, 187 (2015), https://doi.org/10.1186/s11671-015-0896-1
[7] U. Lang, E. Müller, N. Naujoks, and J. Dual, Advanced Functional Materials, **19**, 1215 (2009), https://doi.org/10.1002/adfm.200801258
[8] Y. Lan, Y. Wang, and Y. Song, Flex. Print. Electron. **5**, 014001 (2020), https://doi.org/10.1088/2058-8585/ab5ce3
[9] C. Roldán-Carmona, O. Malinkiewicz, A. Soriano, G.M. Espallargas, A. Garcia, P. Reinecke, T. Kroyer, M. Ibrahim Dar, M. Khaja Nazeeruddin, and H. J. Bolink, Energy & Environmental Science, **7**, 994 (2014), https://doi.org/10.1039/C3EE43619E
[10] T.M. Schmidt, T.T. Larsen-Olsen, J.E. Carlé, D. Angmo, and F.C. Krebs, Advanced Energy Materials, **5**, 1500569 (2015), https://doi.org/10.1002/aenm.201500569
[11] W. Wang, N.R. Paudel, Y. Yan, F. Duarte, and M. Mount, J. Mater. Sci.: Mater. Electron. **27**, 1057 (2016), https://doi.org/10.1007/s10854-015-3850-1
[12] H. Parkhomenko, M. Solovan, A. Mostovyi, K. Ulyanytsky, and P. Maryanchuk, Semiconductors, **51**, 344 (2017). https://doi.org/10.1134/S1063782617030216
[13] M.M. Solovan, N.M. Gavaleshko, V.V. Brus, A.I. Mostovyi, P.D. Maryanchuk, and E. Tresso, Semicond. Sci. Technol. **31**, 105006 (2016), https://doi.org/10.1088/0268-1242/31/10/105006
[14] B.L. Sharma, and R.K. Purohit, *Semiconductor Heterojunctions*, (Elsevier, 2015).
[15] A. Fahrenbruch, and R. Bube, *Fundamentals Of Solar Cells: Photovoltaic Solar Energy Conversion*, (Elsevier, 2012).
[16] Y.J. Lee, C. Yeon, J.W. Lim, and S.J. Yun, Solar Energy, **163**, 398 (2018), https://doi.org/10.1016/j.solener.2018.02.026
[17] A.M. Nardes, M. Kemerink, M.M. de Kok, E. Vinken, K. Maturova, and R.A.J. Janssen, Organic Electronics, **9**, 727 (2008), https://doi.org/10.1016/j.orgel.2008.05.006
[18] L.A. Kosyachenko, X. Mathew, V.V. Motushchuk, and V.M. Sklyarchuk, Solar Energy, **80**, 148 (2006), https://doi.org/10.1016/j.solener.2005.01.009
[19] M.M. Solovan, V.V. Brus, P.D. Maryanchuk, M.I. Ilashchuk, J. Rappich, N. Nickel, and S.L. Abashin, Semicond. Sci. Technol. **29**, 015007 (2013), https://doi.org/10.1088/0268-1242/29/1/015007
[20] S.M. Sze, Y. Li, and K.K. Ng, *Physics of Semiconductor Devices*, (John Wiley & Sons, 2021).
[21] G. a. H. Wetzelaer, M. Kuik, M. Lenes, and P.W.M. Blom, Appl. Phys. Lett. **99**, 153506 (2011), https://doi.org/10.1063/1.3651752
[22] V.V. Brus, P.D. Maryanchuk, M.I. Ilashchuk, J. Rappich, I.S. Babichuk, and Z.D. Kovalyuk, Solar Energy, **112**, 78 (2015), https://doi.org/10.1016/j.solener.2014.11.023
[23] V.V. Brus, and P.D. Maryanchuk, Appl. Phys. Lett. **104**, 173501 (2014), https://doi.org/10.1063/1.4872467
[24] Y. Zhang, P. Huang, J. Guo, R. Shi, W. Huang, Z. Shi, L. Wu, F. Zhang, L. Gao, C. Li, X. Zhang, J. Xu, and H. Zhang, Advanced Materials, **32**, 2001082 (2020), https://doi.org/10.1002/adma.202001082
[25] S. Chakrabarti, A.D. Stiff-Roberts, P. Bhattacharya, S. Gunapala, S. Bandara, S.B. Rafol, and S.W. Kennerly, IEEE Photonics Technology Letters, **16**, 1361 (2004), https://doi.org/10.1109/LPT.2004.825974
[26] V.V. Brus, Semicond. Sci. Technol. **28**, 025013 (2013), https://doi.org/10.1088/0268-1242/28/2/025013
[27] V.V. Brus, A.K.K. Kyaw, P.D. Maryanchuk, and J. Zhang, Progress in Photovoltaics: Research and Applications, **23**, 1526 (2015), https://doi.org/10.1002/pip.2586
[28] J.P. Donnelly and A.G. Milnes, IEEE Transactions on Electron Devices, **14**, 63 (1967), https://doi.org/10.1109/T-ED.1967.15900
[29] V.V. Brus, O.L. Maslyanchuk, M.M. Solovan, P.D. Maryanchuk, I. Fodchuk, V.A. Gnatyuk, N.D. Vakhnyak, S.V. Melnychuk, and T. Aoki, Sci. Rep. **9**, 1065 (2019), https://doi.org/10.1038/s41598-018-37637-w

ЕЛЕКТРИЧНІ ТА ФОТОЕЛЕКТРИЧНІ ВЛАСТИВОСТІ ОРГАНІЧНО-НЕОРГАНІЧНИХ ГЕТЕРОПЕРЕХОДІВ PEDOT:PSS/*n*-CdTe

Г.П. Пархоменко[a], М.М. Солован[a], А.І. Мостовий[a], І.Г. Орлецький[a], В.В. Брус[b]
[a]Кафедра електроніки і енергетики, Чернівецький національний університет імені Юрія Федьковича 58012, Чернівці, Україна
[b]Кафедра фізики, Університет Назарбаєва, 010000, Нур-Султан, Казахстан

Тонкі плівки PEDOT:PSS знайшли широке використання в якості прозорих покритів в гнучких напівпровідникових приладах в тому числі сонячних елементах. Проте вони доволі мало використовуюся в якості просвітлюючих покриттів в поєднанні з кристалічними підкладками. В даній роботі показано можливість використання тонких плівок PEDOT: PSS як фронтального прозорого провідного шару в гібридних органічно-неорганічних гетеропереходах типу Шотткі PEDOT: PSS/*n*-CdTe, які були виготовлені шляхом нанесення тонких плівок PEDOT: PSS (використовуючи метод спінкоутингу) на кристалічні підкладки телуриду кадмію. Виміряно та проаналізовано вольт-амперні (в широкому діапазоні температур) та вольт-фарадні (при кімнатній температурі) характеристики гетеропереходів. Встановлено, що гетеропереходи PEDOT: PSS/*n*-CdTe володіють хорошими діодними властивостями з високим коефіцієнтом випрямлення RR≈10^5, висотою потенціального бар'єру φ_0 = 0,95 еВ та значеннями послідовного R_s = 91 Ом і шунтуючого R_{sh} = 5,7 × 10^7 Ом опорів. Аналіз прямих гілок ВАХ гетеропереходів показав, що домінуючі механізми переносу заряду визначаються процесами випромінювальної рекомбінації при малих зміщеннях (3kT/e <V <0,3 В) та тунелювання через тонкий збіднений шар при великих зміщеннях (0,3 В <V<0,6 В). Вольт-фаратні характеристики побудовані в кординатах Мотта-Шотткі з врахуванням впливу послідовного опору, виміряні при частоті 1 МГц. З ВФХ було визначено величину вбудованого потенціалу V_c= 1,32 В (яка добре корелює з напругою відсічки визначеною з вольт-амперних характеристик) та концентрацію незкомпенсованих донорів у підкладці *n*-CdTe N_D-N_A = 8,79 × 10^{14} $см^{-3}$. Хоча фотоелектричні параметри неоптимізованих гетеропереходів PEDOT:PSS/*n*-CdTe низькі, їх фотодіодні характеристики (детективність D^*> 10^{13} Джонс) є досить перспективними для подальшого детального аналізу та вдосконалення. Запропонована концепція гібридного органічно-неорганічного гетеропереходу типу діода Шотткі, також має потенціал для застосування в недорогих γ- та рентгенівських детекторах.

Ключові слова: PEDOT:PSS, CdTe, гетероперехід, фотодетектор, механізми струмопереносу.